Optics Letters

Optically switchable directional invisibility

ELISA HURWITZ AND GREG GBUR*

Department of Physics and Optical Science, University of North Carolina, Charlotte, North Carolina 28223, USA
**Corresponding author: gjgbur@uncc.edu*

Received 17 January 2017; revised 2 March 2017; accepted 6 March 2017; posted 6 March 2017 (Doc. ID 284726); published 24 March 2017

It is shown that a scatterer can be designed to be directionally invisible for an incident field composed of a given sum of plane waves. These scatterers are invisible only when all plane waves are present with the given amplitudes and directions of incidence, which suggests a new type of "switchable" invisibility. Such objects could find application in optical devices such as couplers, switches, and optical position sensors. It is also demonstrated that the designed scatterers have balanced gain-loss profiles that are more general than most $\mathcal{PT}$-symmetric objects considered so far.

OCIS codes: (290.5839) Scattering, invisibility; (290.5825) Scattering theory; (200.4660) Optical logic.

https://doi.org/10.1364/OL.42.001301

Invisibility has captured the imagination of scientists and fiction writers for ages, but it is only in the last hundred years that it has evolved into a serious possibility. The first hints of invisible objects appeared in pre-quantum theory, and grew out of attempts to explain how the electrons in atoms can accelerate but not radiate power [1,2]. These attempts resulted in the characterization of classical charge-current distributions that do not radiate, known as nonradiating sources [3,4], and these sources were found to be crucial in understanding the uniqueness of the inverse source problem [5].

True invisibility was similarly explored in the context of inverse scattering problems, and it was shown that it is possible to create objects that are directionally invisible for multiple directions of illumination, at least under weak scattering conditions [6]. This work was largely ignored until the possibility of omnidirectional invisibility cloaks was introduced in 2006 [7,8]. Such perfect cloaks require extreme material properties, and there has been a general trend in more recent work toward trading off perfection for material simplicity, for instance, in the use of carpet cloaks [9] or objects with directional invisibility [10,11].

However, it has recently been shown that passive cloaks, which do not possess gain or loss, are inherently bandlimited [12]. Because of this, there has been increasing interest in using active media to construct invisible devices, such as done in [13]. Uni-directionally transparent layered structures have emerged employing parity-time ($\mathcal{PT}$) symmetry as a design strategy [14,15]. With few exceptions [16–18], however, these devices have been one-dimensional. It has been shown recently [19], though, that it is possible to design two- or three-dimensional directionally invisible gain-loss scatterers by using ideas from early nonradiating source theory; these scatterers can not only be designed to be $\mathcal{PT}$-symmetric but also to have no symmetry in their refractive index structure whatsoever [20].

In this Letter, we generalize this method of directional invisibility to theoretically construct objects that are invisible only when simultaneously illuminated by multiple plane waves in given directions. From this, it is suggested that such devices could be used to design novel couplers, switches, and other optical sensors.

Consider an object of refractive index $n(\mathbf{r})$ bounded by a finite surface S and volume V, illuminated by a scalar monochromatic incident field $U^{(i)}(\mathbf{r})$, which may consist of one or more plane waves $U_n(\mathbf{r})$ of different amplitudes:

$$U^{(i)}(\mathbf{r}) = \sum_{n=1}^{N} U_n(\mathbf{r}), \tag{1}$$

where $U_n(\mathbf{r})$ is defined by

$$U_n(\mathbf{r}) = A_n e^{ik\hat{\mathbf{s}}_n\cdot\mathbf{r}}, \tag{2}$$

with A_n representing the amplitude and $\hat{\mathbf{s}}_n$ the direction of the nth plane wave, and $k = \frac{\omega}{c} = \frac{2\pi}{\lambda}$, ω the angular frequency, λ the wavelength, and c representing the vacuum speed of light. The total field $U(\mathbf{r}) = U^{(i)}(\mathbf{r}) + U^{(s)}(\mathbf{r})$, where $U^{(i)}(\mathbf{r})$ and $U^{(s)}(\mathbf{r})$ are the incident and scattered fields, respectively, satisfies the Helmholtz equation with an inhomogeneous wave number:

$$[\nabla^2 + n^2(\mathbf{r})k^2]U(\mathbf{r}) = 0. \tag{3}$$

Introducing the scattering potential $F(\mathbf{r})$ of the form:

$$F(\mathbf{r}) = \frac{k^2}{4\pi}[n^2(\mathbf{r}) - 1], \tag{4}$$

it is possible to write an inhomogeneous wave equation for the scattered field [21]:

$$[\nabla^2 + k^2]U^{(s)}(\mathbf{r}) = -4\pi F(\mathbf{r})U(\mathbf{r}). \tag{5}$$

As the scattered field is present on both sides of Eq. (5), it is not possible to solve this equation analytically. However, we may use it to construct a nonscattering object by following the procedure first presented in [19]. First, we write

$$U^{(s)}(\mathbf{r}) = U^{(i)}(\mathbf{r})U^{(\mathrm{loc})}(\mathbf{r}), \tag{6}$$

where $U^{(\mathrm{loc})}(\mathbf{r})$ is the *local scattered field* of the inhomogeneous scatterer; it is the scattered field with the oscillations of the

incident field removed [19]. Next, we apply techniques promulgated to create *nonradiating sources* [2] to design invisible objects. To this end, the boundary conditions typically employed for nonradiating sources [22] are applied to the local field $U^{(\mathrm{loc})}(\mathbf{r})$ that defines the invisible object, namely,

$$U^{(\mathrm{loc})}(\mathbf{r})|_S = 0, \quad \text{and} \quad \frac{\partial}{\partial n} U^{(\mathrm{loc})}(\mathbf{r})|_S = 0, \tag{7}$$

where $\frac{\partial}{\partial n}$ represents the derivative normal to the surface S, which forms the boundary of the scatterer. The scattered field $U^{(\mathrm{loc})}(\mathbf{r}) = 0$ outside the scatterer. Writing the total field as $U(\mathbf{r}) = [1 + U^{(\mathrm{loc})}(\mathbf{r})]U^{(i)}(\mathbf{r})$, where $U^{(i)}(\mathbf{r})$ is defined by Eq. (1), and substituting it with Eq. (6) into Eq. (5), results in the scattering potential $F(\mathbf{r})$ that produces the scattered field, i.e.,

$$F(\mathbf{r}) = -\frac{1}{4\pi[1 + U^{(\mathrm{loc})}(\mathbf{r})]} \times \left[\nabla^2 U^{(\mathrm{loc})}(\mathbf{r}) + \frac{2ik\sum_{n=1}^{N} U_n(\mathbf{r})\hat{\mathbf{s}}_n \cdot \nabla U^{(\mathrm{loc})}(\mathbf{r})}{\sum_{n=1}^{N} U_n(\mathbf{r})}\right]. \tag{8}$$

For only one incident wave ($N = 1$), the scattering potential is

$$F(\mathbf{r}) = -\frac{1}{4\pi}\frac{\nabla^2 U^{(\mathrm{loc})}(\mathbf{r}) + 2ik\hat{\mathbf{s}}_1 \cdot \nabla U^{(\mathrm{loc})}(\mathbf{r})}{1 + U^{(\mathrm{loc})}(\mathbf{r})}, \tag{9}$$

presented in [19] and explored in more detail in [20].

The general equation [Eq. (8)] for N discrete directions facilitates the design of a scatterer that is invisible for an incident field consisting of multiple plane waves. For two incident waves of different amplitudes, i.e., $N = 2$, the scattering potential is defined by

$$F(\mathbf{r}) = -\frac{1}{4\pi[1 + U^{(\mathrm{loc})}(\mathbf{r})]} \times \left[\nabla^2 U^{(\mathrm{loc})}(\mathbf{r}) + \frac{2ik\hat{\mathbf{s}}_1 \cdot \nabla U^{(\mathrm{loc})}(\mathbf{r})}{1 + \frac{A_2}{A_1} e^{ik(\hat{\mathbf{s}}_2 - \hat{\mathbf{s}}_1)\cdot\mathbf{r}}} + \frac{2ik\hat{\mathbf{s}}_2 \cdot \nabla U^{(\mathrm{loc})}(\mathbf{r})}{1 + \frac{A_1}{A_2} e^{ik(\hat{\mathbf{s}}_1 - \hat{\mathbf{s}}_2)\cdot\mathbf{r}}}\right], \tag{10}$$

where A_1 and A_2 are the amplitudes and $\hat{\mathbf{s}}_1$ and $\hat{\mathbf{s}}_2$ are the directions of incidence of the two plane waves. By choosing $U^{(\mathrm{loc})}(\mathbf{r})$ with appropriate boundary conditions, and the amplitudes and directions of incidence for the plane waves, we uniquely specify the form of $F(\mathbf{r})$ with the desired invisibility properties. For example, let us choose a circular object of radius a with

$$U^{(\mathrm{loc})}(\mathbf{r}) = \cos^2\left(\frac{\pi r^2}{2a^2}\right), \tag{11}$$

where $r = \sqrt{x^2 + y^2}$, $a = 1$, $A_1 = 1$, $A_2 = 20$, $\hat{\mathbf{s}}_1 = \hat{\mathbf{x}}$, and $\hat{\mathbf{s}}_2 = \hat{\mathbf{y}}$. This choice of $U^{(\mathrm{loc})}$ provides a simple example, but any $U^{(\mathrm{loc})}$ that satisfies Eq. (7) may be chosen. The incident field is defined by Eq. (1) with $N = 2$ such that

$$U^{(i)}(\mathbf{r}) = A_1 e^{ik\hat{\mathbf{s}}_1\cdot\mathbf{r}} + A_2 e^{ik\hat{\mathbf{s}}_2\cdot\mathbf{r}}. \tag{12}$$

Numerical simulations of waves interacting with this directionally nonscattering scatterer were performed using a Green's function method [23] for two cases. First, the fields were calculated when both components of the incident field given by Eq. (12) were present. Then the total and scattered fields were calculated when only one of the components of the incident field was present. The scattering potential is found by substituting Eq. (11) into Eq. (10). While the real part has a more balanced amplitude in both the $\hat{\mathbf{x}}$ and $\hat{\mathbf{y}}$ directions, the imaginary part is roughly antisymmetric along the $\hat{\mathbf{y}}$ axis and has an amplitude range roughly twice as large as the real component (Fig. 1). This emphasizes the roles gain and loss play in these invisible objects. Because the local scattered field $U^{(\mathrm{loc})}(\mathbf{r})$ was taken to be real and symmetric, the scattering potential possesses the conjugate inversion symmetry $F(\mathbf{r}) = F^{\star}(-\mathbf{r})$. This is a very general example of $\mathcal{PT}$ symmetry; most examples of $\mathcal{PT}$ symmetry that have been studied to date focus on structures that also have this conjugate symmetry with respect to a single axis, i.e., $F(x, y, z) = F^{\star}(-x, y, z)$, which our structure does not have. More generally, by choosing a $U^{(\mathrm{loc})}$, which is not real or symmetric, it is possible to produce structures that do not possess any symmetry in their potential. These directional invisible objects are active gain-loss scatterers with balanced gain and loss.

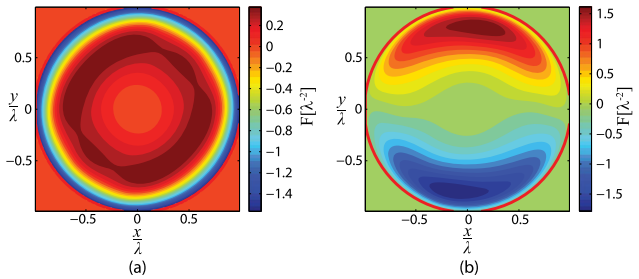

Fig. 1. Real (a) and imaginary (b) parts of $F(\mathbf{r})$ [Eq. (10)] with $U^{(\mathrm{loc})}(\mathbf{r})$ [Eq. (11)] with $a = 1$, $A_1 = 1$, $A_2 = 20$, $\hat{\mathbf{s}}_1 = \hat{\mathbf{x}}$, and $\hat{\mathbf{s}}_2 = \hat{\mathbf{y}}$.

When both of the components of the incident fields are present, the nonscattering scatterer is invisible (Fig. 2). The incident fields appear undisturbed outside the scatterer [Fig. 2(a)]. This is further confirmed in that the scattered field outside the scatterer is identically zero [Fig. 2(b)]. However, if one of the components of the incident field is removed, or incident from a different direction, there is significant scattering, as we will now illustrate. Figure 3(a) shows the scattered field when a field is incident only in the $\hat{\mathbf{x}}$-direction. Figure 3(b) shows the scattered field when an incident field propagates only in the $\hat{\mathbf{y}}$-direction. In both cases, there is a strong scattered field. Therefore, this kind of scatterer is invisible only when both waves are incident in their respective directions simultaneously

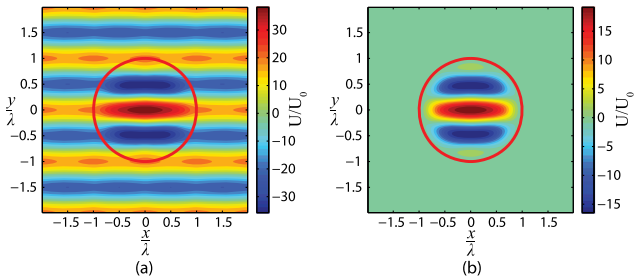

Fig. 2. Real parts of the $U(\mathbf{r})$ (a) and $U^{(s)}(\mathbf{r})$ (b) invisible to $U^{(i)}(\mathbf{r})$ [Eq. (12)] with $F(\mathbf{r})$ [Eq. (10)] with $a = 1$, $A_1 = 1$, $A_2 = 20$, $\hat{\mathbf{s}}_1 = \hat{\mathbf{x}}$, and $\hat{\mathbf{s}}_2 = \hat{\mathbf{y}}$.

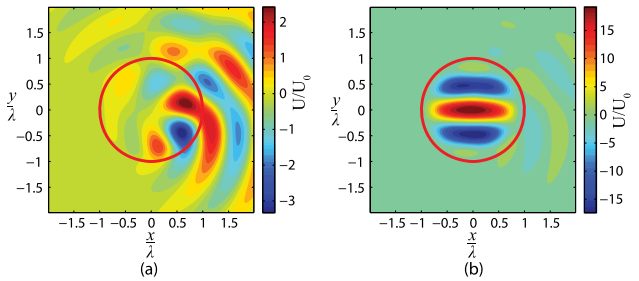

Fig. 3. Real part of $U^{(s)}(\mathbf{r})$ when $U^{(i)}(\mathbf{r})$ is incident in either (a) $\hat{\mathbf{x}}$ or (b) $\hat{\mathbf{y}}$, for an object invisible to $U^{(i)}(\mathbf{r})$ [Eq. (12)]. $F(\mathbf{r})$ [Eq. (10)] has $a = 1$, $A_1 = 1$, $A_2 = 20$, $\hat{\mathbf{s}}_1 = \hat{\mathbf{x}}$, and $\hat{\mathbf{s}}_2 = \hat{\mathbf{y}}$.

with the proper amplitudes. Because this nonscattering scatterer is invisible only if the incident field comprises specific plane waves with designated directions and amplitudes, one could imagine building an optically switchable coupler with this device, where one field is the "pump" and the other field is the "probe." While the pump is held at the designed magnitude and direction, the probe might be varied. The device transmits both fields perfectly only when the probe is also set to the correct amplitude and direction.

To explore this switching effect further, we consider the power extinguished and scattered by the object as the amplitude of the probe is varied. The extinguished power $P^{(\text{ext})}$ is defined as the power removed from the incident field by the scatterer (Chapter 2 in Ref. [24]) (and can be derived from [21]), and is given by

$$P^{(\text{ext})} = -\frac{1}{2ik}\int_L (U^{(i)\star}\nabla U^{(s)} + U^{(s)\star}\nabla U^{(i)} - \text{c.c.})\cdot\hat{\mathbf{n}}\,dl \tag{13}$$

and c.c. refers to the complex conjugate. The scattered power $P^{(\text{sca})}$ is defined as the total integrated power scattered by the object (Chapter 2 in Refs. [21,24]), and is given by

$$P^{(\text{sca})} = \frac{1}{2ik}\int_L (U^{(s)\star}\nabla U^{(s)} - U^{(s)}\nabla U^{(s)\star})\cdot\hat{\mathbf{n}}\,dl. \tag{14}$$

We may also introduce the power absorbed by the object as $P^{(\text{abs})}$ [21]; it is related to $P^{(\text{ext})}$ and $P^{(\text{sca})}$ by

$$P^{(\text{ext})} = P^{(\text{sca})} + P^{(\text{abs})}. \tag{15}$$

In the presence of gain, $P^{(\text{abs})}$ may be negative, as shown by Kerker [25]; it is therefore possible to have a gain object with zero extinguished power but nonzero scattered power. This is the case in which one of the incident field components is omitted (Fig. 3); $P^{(\text{sca})} \approx 6.6$ when either the $\hat{\mathbf{x}}$ or the $\hat{\mathbf{y}}$ component was present, while $P^{(\text{ext})} = 0$.

True invisibility occurs only when $P^{(\text{abs})}$ and $P^{(\text{ext})}$ are simultaneously zero [25]. Normalized versions of these quantities are shown in Fig. 4 as a function of the ratio A/A_2, where A is the probe field amplitude and A_2 is the value of the probe field amplitude at which it has been designed to be invisible. $P^{(\text{sca})}$ and $P^{(\text{ext})}$ have been normalized by $A_1^2 + A^2$, which is the average power per unit length of the incident field. It can be seen that both quantities are simultaneously zero only when $A/A_2 = 1$.

To study the effect of relative phase between the incident field components on invisibility, a phase between 0 and $\pi/2$ was added to one of the components, and $P^{(\text{ext})}$ and $P^{(\text{sca})}$ were

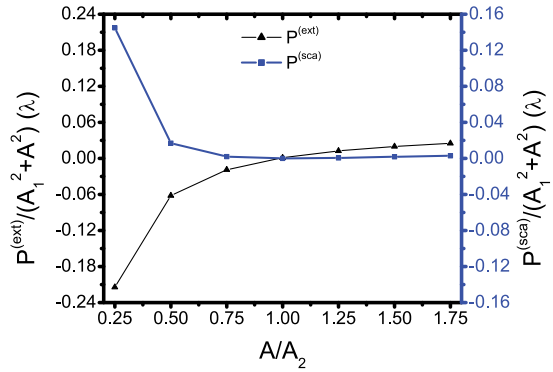

Fig. 4. $P^{(\text{ext})}$ and $P^{(\text{sca})}$ versus the ratio A/A_2. $A = A_2$ is the value of the probe field at which the object is invisible.

calculated normalized by $A_1^2 + A_2^2$. All of the calculated values were below 10%, indicating that this type of scatterer is resilient in the presence of a relative phase change.

A scatterer can also be designed for a field with three or more directions of incidence. For example, if $N = 3$ in Eq. (8), the scattering potential is given by

$$\begin{aligned} F(\mathbf{r}) = -\frac{1}{4\pi[1 + U^{(\text{loc})}(\mathbf{r})]}\times\Bigg[&\nabla^2 U^{(\text{loc})}(\mathbf{r}) \\ &+ \frac{2ik\hat{\mathbf{s}}_1\cdot\nabla U^{(\text{loc})}(\mathbf{r})}{1 + \frac{A_2}{A_1}e^{ik(\hat{\mathbf{s}}_2-\hat{\mathbf{s}}_1)\cdot\mathbf{r}} + \frac{A_3}{A_1}e^{ik(\hat{\mathbf{s}}_3-\hat{\mathbf{s}}_1)\cdot\mathbf{r}}} \\ &+ \frac{2ik\hat{\mathbf{s}}_2\cdot\nabla U^{(\text{loc})}(\mathbf{r})}{1 + \frac{A_1}{A_2}e^{ik(\hat{\mathbf{s}}_1-\hat{\mathbf{s}}_2)\cdot\mathbf{r}} + \frac{A_3}{A_2}e^{ik(\hat{\mathbf{s}}_3-\hat{\mathbf{s}}_2)\cdot\mathbf{r}}} \\ &+ \frac{2ik\hat{\mathbf{s}}_3\cdot\nabla U^{(\text{loc})}(\mathbf{r})}{1 + \frac{A_1}{A_3}e^{ik(\hat{\mathbf{s}}_1-\hat{\mathbf{s}}_3)\cdot\mathbf{r}} + \frac{A_2}{A_3}e^{ik(\hat{\mathbf{s}}_2-\hat{\mathbf{s}}_3)\cdot\mathbf{r}}}\Bigg], \end{aligned} \tag{16}$$

where A_1, A_2, A_3 are the amplitudes and $\hat{\mathbf{s}}_1$, $\hat{\mathbf{s}}_2$, $\hat{\mathbf{s}}_3$, are the directions of incidence of the incident field $U^{(i)}(\mathbf{r})$, given by

$$U^{(i)}(\mathbf{r}) = A_1 e^{ik\hat{\mathbf{s}}_1\cdot\mathbf{r}} + A_2 e^{ik\hat{\mathbf{s}}_2\cdot\mathbf{r}} + A_3 e^{ik\hat{\mathbf{s}}_3\cdot\mathbf{r}}. \tag{17}$$

Two tri-directional scatterers were designed using the local scattered field given by Eq. (11). The first one is invisible for fields simultaneously incident in the $\hat{\mathbf{s}}_1 = \hat{\mathbf{x}}$, $\hat{\mathbf{s}}_2 = \hat{\mathbf{y}}$, and in the $\hat{\mathbf{s}}_3 = \hat{\mathbf{x}} - \hat{\mathbf{y}}$ directions. The following values were used for the incident fields: $A_1 = 1$, $A_2 = 1$, and $A_3 = 5$. Again, the real part of the scattering potential exhibits inversion symmetry, while its imaginary part has inversion anti-symmetry (Fig. 5). The scattered field for this tri-directionally invisible scatterer is shown for when the incident fields are propagating in the invisibility directions [Fig. 6(a)]. When the field in the $\hat{\mathbf{y}}$ direction instead propagates in the $-\hat{\mathbf{y}}$ direction, the scatterer is no longer invisible [Fig. 6(b)].

Such a scatterer can also be designed with counter-propagating pump fields. The second tri-directional nonscattering scatterer is invisible for fields simultaneously incident in the $\hat{\mathbf{s}}_1 = \hat{\mathbf{x}}$, $\hat{\mathbf{s}}_2 = \hat{\mathbf{y}}$, and in the $\hat{\mathbf{s}}_3 = -\hat{\mathbf{x}}$ directions with amplitudes $A_1 = 1$, $A_2 = 2$, and $A_3 = 5$. It is of note that the scattering potential in this case has also the aforementioned inversion symmetry. The real part of the scattered field for this tri-directionally invisible scatterer is shown in Fig. 7(a) for the case in which the incident fields all propagate in the invisibility direction. This shows that it is possible to design directionally

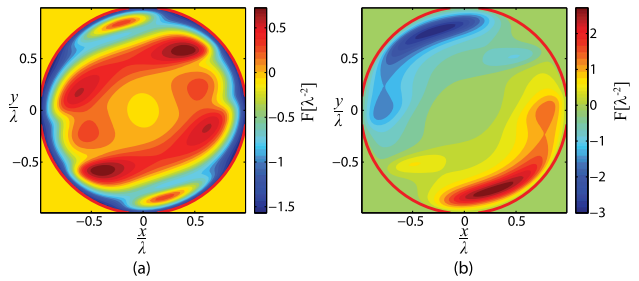

Fig. 5. Real (a) and imaginary (b) parts of $F(\mathbf{r})$ [Eq. (16)] with $U^{(\mathrm{loc})}(\mathbf{r})$ [Eq. (11)] with $a = 1$, and $A_1 = 1$, $A_2 = 1$, $A_3 = 5$, $\hat{\mathbf{s}}_1 = \hat{\mathbf{x}}$, $\hat{\mathbf{s}}_2 = \hat{\mathbf{y}}$, and $\hat{\mathbf{s}}_3 = \hat{\mathbf{x}} - \hat{\mathbf{y}}$.

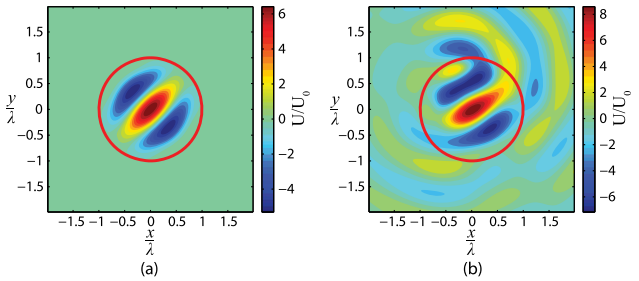

Fig. 6. Real part of $U^{(s)}(\mathbf{r})$ with $U^{(i)}(\mathbf{r})$ [Eq. (17)] and (a) $\hat{\mathbf{s}}_2 = \hat{\mathbf{y}}$ (invisibility) or (b) $\hat{\mathbf{s}}_2 = -\hat{\mathbf{y}}$. $F(\mathbf{r})$ is given by Eq. (16) with $a = 1$, $A_1 = 1$, $A_2 = 1$, $A_3 = 5$, $\hat{\mathbf{s}}_1 = \hat{\mathbf{x}}$, $\hat{\mathbf{s}}_2 = \hat{\mathbf{y}}$, and $\hat{\mathbf{s}}_3 = \hat{\mathbf{x}} - \hat{\mathbf{y}}$.

invisible scatterers using this method with unequal amplitudes in opposite directions. If the third incident field has $\hat{\mathbf{s}}_3 = -\hat{\mathbf{x}} + \hat{\mathbf{y}}$ instead of its given direction, the scatterer no longer is invisible and scatters in response to the incident field [Fig. 7(b)].

Though we have focused here on the scalar wave equation for simplicity, the same methods may be applied to electromagnetic waves, as was shown in [19]. For a non-magnetic material, one uses the vector wave equation for the electric field $\mathbf{E}$:

$$\nabla \times (\nabla \times \mathbf{E}^{(s)}) - k^2 \mathbf{E}^{(s)} = -4\pi \mathbf{F} \cdot \mathbf{E}, \tag{18}$$

where $\mathbf{F}$ is a generally anisotropic scattering potential based on the permittivity. The same conditions for the scalar field in Eq. (7) may be used for the electric field $\mathbf{E}$ to make an invisible object.

The examples here have a scattering potential that varies continuously in space, which in practice will be difficult to fabricate. However, because Eq. (8) for the scattering potential depends in a simple way upon the derivatives of the chosen local field, it should be possible to make a more sophisticated choice of $U^{(\mathrm{loc})}$ that will provide a simpler, even piecewise constant, potential. The only conditions that $U^{(\mathrm{loc})}$ must satisfy are continuity of the field and its derivative throughout the volume and Eq. (7) on the boundary, which provides much freedom.

This method could be used to design a variety of novel, directional optical devices, for example, an optically switchable, directionally invisible, optical coupler. It is also possible to imagine an optical lock or switch that will transmit at the right power and direction only if all beams are present at the same time. Such a device might also be combined with an optical detector, designed to detect only a specific incident field composed of the sum of plane waves. These kinds of devices could

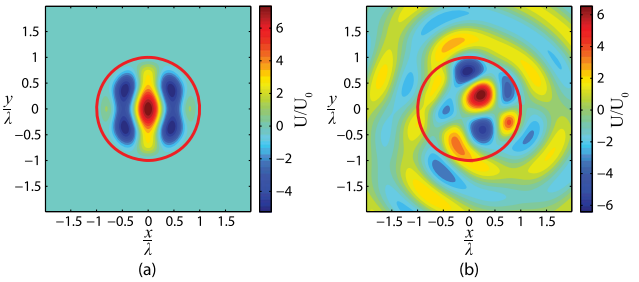

Fig. 7. Real part of $U^{(s)}(\mathbf{r})$ for $U^{(i)}(\mathbf{r})$ [Eq. (17)] and (a) $\hat{\mathbf{s}}_3 = -\hat{\mathbf{x}}$ (invisibility) or (b) with $\hat{\mathbf{s}}_3 = -\hat{\mathbf{x}} + \hat{\mathbf{y}}$. $F(\mathbf{r})$ [Eq. (16)] has $a = 1$, $A_1 = 1$, $A_2 = 2$, $A_3 = 5$, $\hat{\mathbf{s}}_1 = \hat{\mathbf{x}}$, $\hat{\mathbf{s}}_2 = \hat{\mathbf{y}}$, and $\hat{\mathbf{s}}_3 = -\hat{\mathbf{x}}$.

also be used to improve efficiency of solar cells and thermophotovoltaic cells, in which light incident in a number of directions simultaneously will be transmitted with minimal reflection.

Since the Helmholtz equation is analogous to the time-independent Schrödinger equation, the technique here can also be applied to quantum mechanics by applying the boundary conditions to the quantum wave function. This implies that there is a broader class of quantum potentials for which the Hamiltonian has real energy eigenvalues.

REFERENCES

1. A. Sommerfeld, Nachr. Ges. Wiss. Goettingen, Math. Phys. Kl. **1904**, 99 (1904).
2. G. Gbur, *Progress in Optics*, E. Wolf, ed. (Elsevier, 2003), Vol. **45**, pp. 273–315.
3. P. Ehrenfest, Phys. Unserer Zeit **11**, 708 (1910).
4. G. A. Schott, London Edinburgh Dublin Philos. Mag. J. Sci. **15**(100), 752 (1933).
5. F. Friedlander, Proc. London Math. Soc. **s3**, 551 (1973).
6. A. J. Devaney and E. Wolf, Phys. Rev. D **8**, 1044 (1973).
7. U. Leonhardt, Science **312**, 1777 (2006).
8. J. B. Pendry, D. Schurig, and D. R. Smith, Science **312**, 1780 (2006).
9. M. Gharghi, C. Gladden, T. Zentgraf, Y. Liu, X. Yin, J. Valentine, and X. Zhang, Nano Lett. **11**, 2825 (2011).
10. M. C. Zheng, D. N. Christodoulides, R. Fleischmann, and T. Kottos, Phys. Rev. A **82**, 010103 (2010).
11. L. Feng, Y.-L. Xu, W. Fegadolli, M.-H. Lu, J. Oliveira, V. Almeida, Y.-F. Chen, and A. Scherer, Nat. Mater. **12**, 108 (2012).
12. F. Monticone and A. Alù, Optica **3**, 718 (2016).
13. D. A. B. Miller, Opt. Express **14**, 12457 (2006).
14. C. Rüter, K. Makris, R. El-Ganainy, D. Christodoulides, M. Segev, and D. Kip, Nat. Phys. **6**, 192 (2010).
15. Z. Lin, H. Ramezani, T. Eichelkraut, T. Kottos, H. Cao, and D. N. Christodoulides, Phys. Rev. Lett. **106**, 213901 (2011).
16. X. Zhu, L. Feng, P. Zhang, X. Yin, and X. Zhang, Opt. Lett. **38**, 2821 (2013).
17. D. L. Sounas, R. Fleury, and A. Alù, Phys. Rev. Appl. **4**, 014005 (2015).
18. P. Ambichl, K. G. Makris, L. Ge, Y. Chong, A. D. Stone, and S. Rotter, Phys. Rev. X **3**, 041030 (2013).
19. G. Gbur, Opt. Lett. **40**, 986 (2015).
20. E. Hurwitz and G. Gbur, Phys. Rev. A **93**, 041803 (2016).
21. M. Born and E. Wolf, *Principles of Optics*, 7th ed. (Cambridge University, 1999).
22. A. Gamliel, K. Kim, A. I. Nachman, and E. Wolf, J. Opt. Soc. Am. A **6**, 1388 (1989).
23. O. J. F. Martin and N. B. Piller, Phys. Rev. E **58**, 3909 (1998).
24. S. Carney, "Optical theorems in statistical wavefields with applications," Ph.D. dissertation (University of Rochester, 1999).
25. M. Kerker, Appl. Opt. **17**, 3337 (1978).